

Dielectric and piezoelectric properties of $K_{0.5}Na_{0.5}NbO_3-AgSbO_3$ lead-free ceramics

Dunmin Lin,^{a)} K. W. Kwok, and H. L. W. Chan

Department of Applied Physics and Materials Research Centre, The Hong Kong Polytechnic University, Kowloon, Hong Kong, China

(Received 25 April 2009; accepted 27 June 2009; published online 3 August 2009)

Lead-free piezoelectric ceramics $(1-x)K_{0.5}Na_{0.5}NbO_3-xAgSbO_3+0.75$ mol % MnO_2 were prepared by a conventional solid-state sintering technique, and the piezoelectric and dielectric properties of the ceramics were studied. The results of x-ray diffraction suggest that $AgSbO_3$ diffuses into the $K_{0.5}Na_{0.5}NbO_3$ lattices to form a new solid solution with a single-phase orthorhombic perovskite structure. After the addition of $AgSbO_3$, the paraelectric cubic-ferroelectric tetragonal phase transition temperature (T_C) and the ferroelectric tetragonal-ferroelectric orthorhombic phase transition temperature (T_{O-T}) decrease, and the ceramics become “softened,” resulting in significant improvements in the ferroelectric and piezoelectric properties. The ceramics with $x=0.03-0.10$ exhibit excellent piezoelectric properties: $d_{33}=130-216$ pC/N, $k_p=0.44-0.51$, and $k_t=0.40-0.52$. The ceramics also exhibit a good thermal stability up to high T_{O-T} , suggesting that the ceramics are promising candidates for lead-free piezoelectric ceramics. © 2009 American Institute of Physics. [DOI: 10.1063/1.3186039]

I. INTRODUCTION

Lead-based piezoelectric ceramics, represented by $Pb(Ti,Zr)O_3$ and $Pb(Ti,Zr)O_3$ -based multicomponent ceramics, are widely used in actuators, sensors, as well as microelectronic devices due to their excellent ferroelectric and piezoelectric properties. However, due to the high toxicity of lead oxide and its high vapor pressure during sintering, the use of lead-based ceramics has caused serious environmental problems. Therefore, there is a great need to develop lead-free piezoelectric ceramics with good piezoelectric properties for replacing the lead-based ceramics in various applications.

$K_{0.5}Na_{0.5}NbO_3$ (KNN), the solid solution of ferroelectric $KNbO_3$ and antiferroelectric $NaNbO_3$, has been studied extensively and is considered one of the most promising candidates for lead-free piezoelectric ceramics because of its high Curie temperature, good ferroelectric properties, and large electromechanical coupling coefficients.¹⁻³ A dense and well-sintered KNN ceramic (e.g., prepared by the hot-pressing technique) possesses high density ($\rho=4.46$ g/cm³) and good piezoelectric properties (piezoelectric coefficient $d_{33}=160$ pC/N and planar-mode electromechanical coupling coefficient $k_p=0.45$).¹ However, because of the high volatility of alkaline elements at high temperatures, it is very difficult to obtain dense and well-sintered KNN ceramics using a conventional sintering process, and the ceramics usually exhibit worse piezoelectric properties ($d_{33}=80$ pC/N, $k_p=0.36$, and $\rho=4.25$ g/cm³).^{2,3} A number of studies have been carried out to improve the sinterability and properties of KNN ceramics; these include the formation of solid solutions of KNN with other ABO_3 -type ferroelectrics or nonferroelectrics [e.g., $LiNbO_3$,⁴ $Bi_{0.5}Na_{0.5}TiO_3$,⁵ $BaTiO_3$,⁶ $SrTiO_3$,⁷ $LiTaO_3$,⁸ and $LiSbO_3$ (Ref. 9)], the substitutions of analogous ions (e.g., Li^+ , Sb^{5+} , and Ta^{5+}) for the A-site K^+ and

Na^+ or the B-site Nb^{5+} ions,^{10,11} and the use of sintering aids [e.g., CuO (Ref. 12) and $K_{5.4}Cu_{1.3}Ta_{10}O_{29}$ (Ref. 13)]. In the present work, a new solid solution $K_{0.5}Na_{0.5}NbO_3-AgSbO_3$ was developed and prepared by conventional solid-state sintering, and their piezoelectric and dielectric properties were studied. On the basis of our previous work,¹⁴ 0.75 mol% MnO_2 , acting as a sintering aid, was added to the ceramics in order to improve the densification of the ceramics.

II. EXPERIMENTAL PROCEDURE

$(1-x)K_{0.5}Na_{0.5}NbO_3-xAgSbO_3+0.75$ mol % MnO_2 (KNN-AS-x) ceramics were prepared by a conventional solid-state sintering technique using analytical-grade metal oxides or carbonate powders: Na_2CO_3 (99.8%), K_2CO_3 (99.9%), Ag_2O (99%), Sb_2O_3 (99%), Nb_2O_5 (99.95%), and MnO_2 (99%). The powders in the stoichiometric ratio of the composition were mixed thoroughly in ethanol using zirconia balls for 8 h, and then dried and calcined at 880 °C for 6 h. After the calcination, MnO_2 was added. The resulting mixture was ball milled again for 8 h and mixed thoroughly with a polyvinyl alcohol (PVA) binder solution, and then pressed into disk samples. The disk samples were finally sintered at 1100 °C for 4 h in air. Silver electrodes were fired on the top and bottom surfaces of the samples. The ceramics were poled under a dc field of 5–6 kV/mm at 100 °C in a silicon oil bath for 30 min.

The crystallite structure of the sintered samples was examined using x-ray diffraction (XRD) analysis with $Cu K\alpha$ radiation (Bruker D8 Advance). The microstructures were observed using a scanning electron microscope (SEM) (JSM-5900LV). The relative permittivity ϵ_r and loss tangent $\tan \delta$ were measured as a function of temperature using an impedance analyzer (Agilent 4192A). A conventional Sawyer-Tower circuit was used to measure the polarization hysteresis ($P-E$) loop at 100 Hz. The electromechanical coupling coef-

^{a)}Electronic mail: ddmd222@yahoo.com.cn

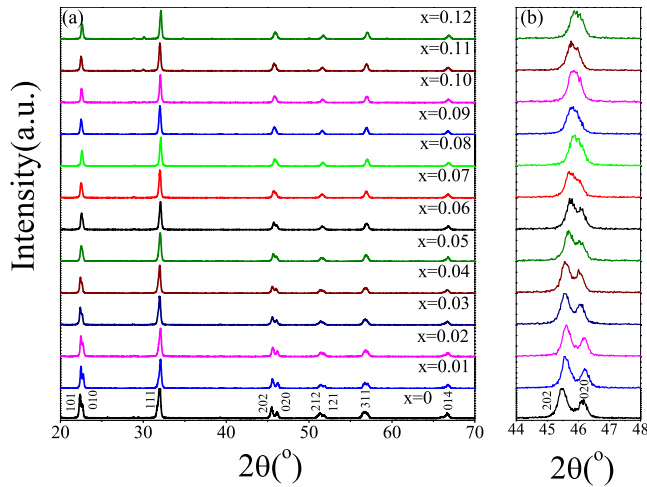


FIG. 1. (Color online) XRD patterns of the KNN-AS- x ceramics.

ficients k_p and k_t and mechanical quality factor Q_m were determined by the resonance method according to the IEEE Standards using an impedance analyzer (Agilent 4294A). The piezoelectric coefficient d_{33} was measured using a piezo- d_{33} meter (ZJ-3A, China).

III. RESULTS AND DISCUSSION

The XRD patterns of the KNN-AS- x ceramics are shown in Fig. 1. Similar to the KNN ceramic,¹⁻³ all the KNN-AS- x ceramics possess a single-phase perovskite structure with orthorhombic symmetry and no secondary phase is observed [Fig. 1(a)]. This suggests that AgSbO_3 has diffused into the KNN lattices to form a new solid solution, with Ag^+ entering the $(\text{K}_{0.5}\text{Na}_{0.5})^+$ sites and Sb^{5+} occupying the Nb^{5+} sites. As shown in Fig. 1(b), the two diffraction peaks (202) and (020) start to merge together at $x > 0.08$. It seems that the ceramic has a tendency to transform into another phase, e.g., pseudocubic, at high AS concentrations. However, it is suggested that the crystal structure of the ceramic should remain orthorhombic, probably with similar lattice constants a , b , and c . Similar results have been observed for the Ta-modified KNN ceramics.¹⁰ By measuring the temperature dependences of the relative permittivity ϵ_r of the ceramics, additional experimental data of phase transition will be provided for further discussion in the following paragraphs.

Figure 2 shows the SEM micrographs of the fracture surfaces of the KNN-AS- x ceramics with $x=0.02$, 0.08, and 0.12. All the ceramics are well sintered and possess a dense microstructure. For the ceramics with larger x , the grains become smaller and more uniform in size. The ceramics also exhibit a well-saturated and squarelike P - E hysteresis loop under an electric field of about 6 kV/mm. Figure 3 shows, as examples, the P - E loops of the KNN-AS- x ceramics with $x=0$, 0.04, 0.08, and 0.12, while the variations in the remanent polarization P_r and coercive field E_c with x are shown in Fig. 4. Both the observed P_r and E_c increase and then decrease with increasing x , giving the maximum values of $29.0 \mu\text{C}/\text{cm}^2$ and $1.15 \text{ kV}/\text{mm}$, respectively, at $x=0.03$. Unlike P_r , the dependence of E_c on x is relatively weak.

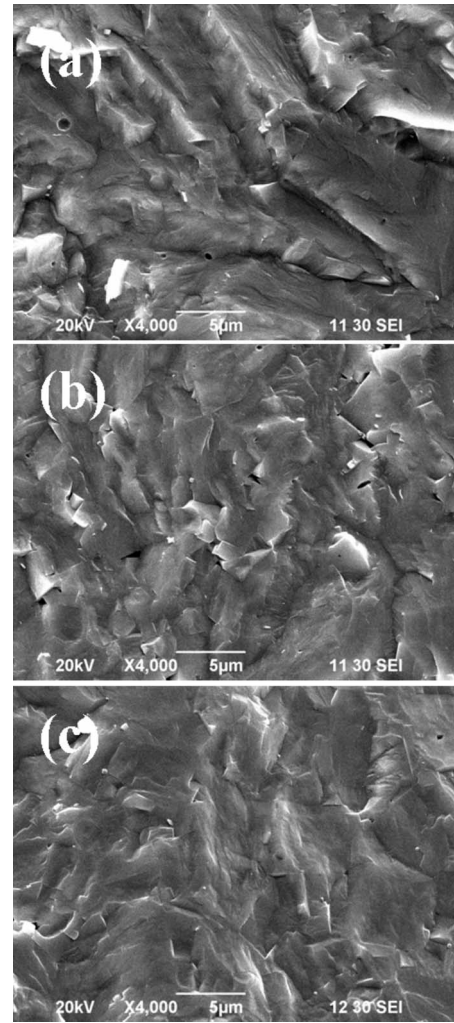


FIG. 2. SEM micrographs of the fracture surfaces of the KNN-AS- x ceramics.

The variations in d_{33} , k_p , k_t , ϵ_r , $\tan \delta$, and Q_m with x for the KNN-AS- x ceramics are shown in Fig. 5. The observed d_{33} increases significantly from 106 to 216 pC/N as x increases from 0 to 0.09, and then decreases at larger x . Unlike d_{33} , the observed k_p and k_t increase only slightly with increasing x , giving maximum values of 0.51 and 0.52, respec-

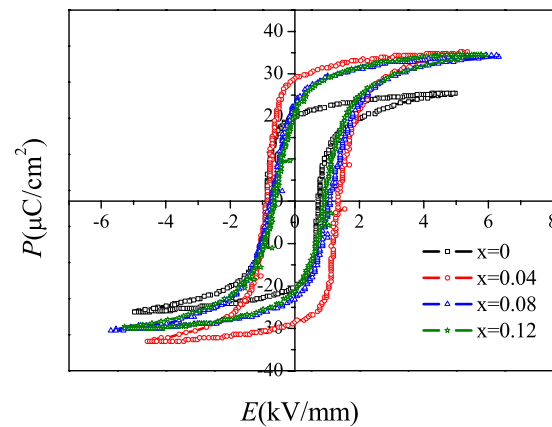


FIG. 3. (Color online) P - E hysteresis loop of the KNN-AS- x ceramics with $x=0$, 0.04, 0.08, and 0.12.

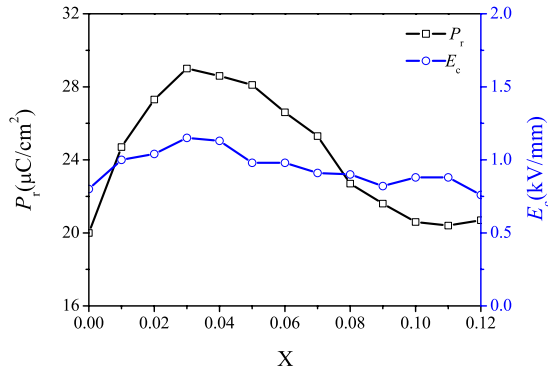


FIG. 4. (Color online) Variations in P_r and E_c with x for the KNN-AS- x ceramics.

tively, at $x=0.04$. The observed ϵ_r increases significantly from 310 to 1690 as x increases from 0 to 0.12. The observed $\tan \delta$ remains at a value smaller than 3% at $x < 0.06$, and then increases significantly to about 10% at $x=0.12$. Unlike the other material parameters, the observed Q_m decreases significantly from 441 to 71 as x increases from 0 to 0.12. On the basis of the above results, it can be seen that the ceramics are “softened” after the addition of AS. Sb has a much larger Pauling electronegativity than Nb (2.05 versus 1.5). Therefore, the partial substitution of Sb^{5+} for Nb^{5+} in the KNN-AS- x ceramics induces a much stronger covalence which favors the piezoelectricity and ferroelectricity.¹¹

The temperature dependences of ϵ_r and $\tan \delta$ for the KNN-AS- x ceramics with $x=0, 0.02, 0.04, 0.06, 0.08, 0.10,$ and 0.12 are shown in Fig. 6. Similar to a pure KNN ceramic,^{1–3} the ceramic with $x=0$ undergoes the cubic-tetragonal phase transition at 429°C (T_C) and the tetragonal-orthorhombic phase transition at 202°C (T_{O-T}). It should be noted that KNN will undergo another transition from the orthorhombic to rhombohedral phase at -200°C ,¹⁵ which is not in the temperature range of the present investigation. As shown in Fig. 6, after the addition of AgSbO_3 , the ceramics

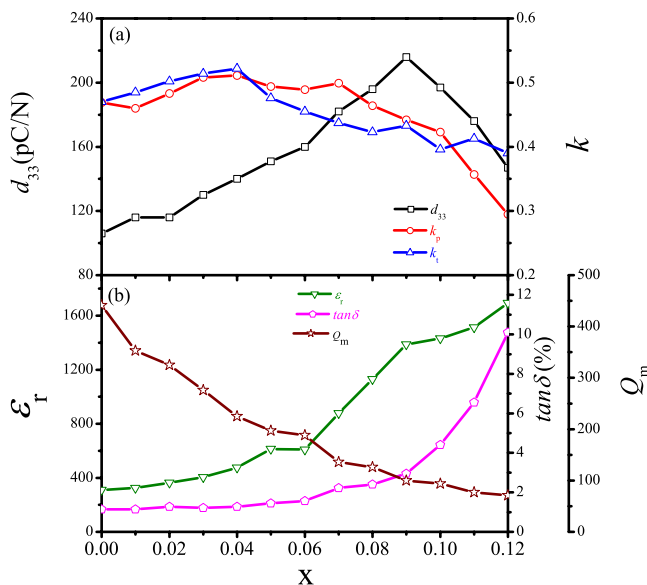


FIG. 5. (Color online) Variations in d_{33} , k_t , k_p , ϵ_r , $\tan \delta$, and Q_m with x for the KNN-AS- x ceramics.

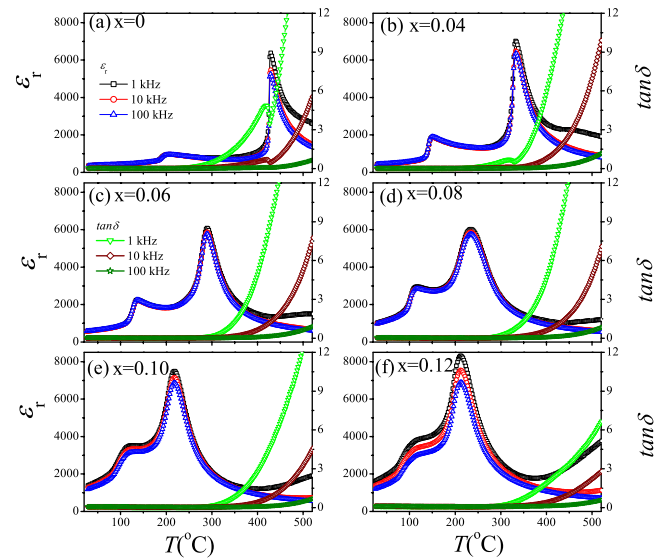


FIG. 6. (Color online) Temperature dependences of ϵ_r and $\tan \delta$ (at 1, 10, and 100 kHz) for the KNN-AS- x ceramics with $x=0, 0.04, 0.06, 0.08, 0.10,$ and 0.12 .

undergo the cubic-tetragonal and tetragonal-orthorhombic phase transitions, with both T_C and T_{O-T} shifted to lower temperatures. Figure 7 shows the variations in T_C and T_{O-T} with x for the KNN-AS- x ceramics. The observed T_C decreases significantly from 425 to 215°C as x increases from 0 to 0.09 and then remains almost unchanged at larger x . Similar to T_C , the observed T_{O-T} decreases significantly from 202 to 114°C as x increases from 0 to 0.08, and then remains almost unchanged. On the basis of the results, it can be seen that all the ceramics should have an orthorhombic structure at room temperature. This provides additional evidence for the suggestion that the crystal structure of the ceramics with $x > 0.08$ should remain orthorhombic although their (room-temperature) diffraction peaks (202) and (020) merge into one [Fig. 1(b)].

As also shown in Fig. 6, the transition peak associated with the cubic-tetragonal phase transition becomes broadened at $x \geq 0.04$. This suggests that a diffuse phase transition is induced. A diffuse phase transition has been observed in many ABO_3 -type perovskites and bilayer structure compounds such as $\text{Ba}_{0.5}\text{Na}_{0.5}\text{TiO}_3$ -based ceramics,¹⁶ $\text{K}_{0.5}\text{La}_{0.5}\text{Bi}_2\text{Nb}_2\text{O}_9$,¹⁷ Na-modified La-doped PZT,¹⁸ $\text{Pb}(\text{Mg}_{1/3}\text{Nb}_{2/3})\text{O}_3$,¹⁹ and KNN-SrTiO₃.²⁰ It has been known

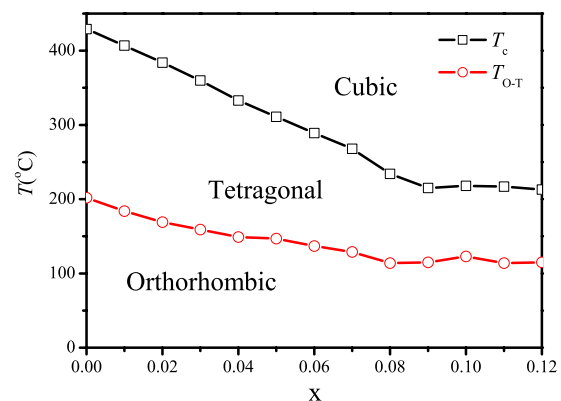


FIG. 7. (Color online) Phase diagrams of the KNN-AS- x ceramics.

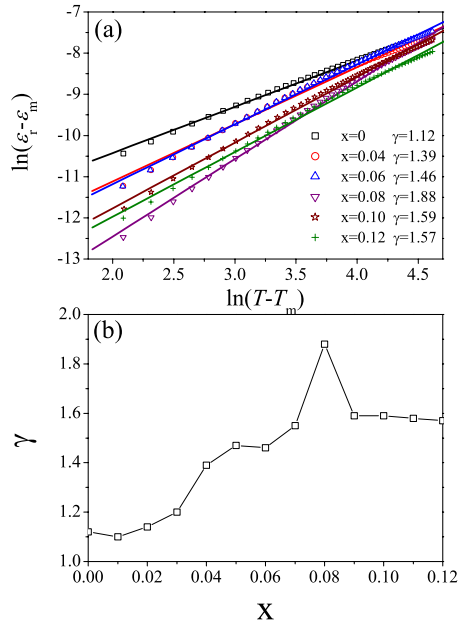


FIG. 8. (Color online) (a) Plot of $\log(1/\epsilon_r - 1/\epsilon_m)$ vs $\log(T - T_m)$ for the KNN-AS- x ceramics with $x=0, 0.04, 0.06, 0.08, 0.10,$ and 0.12 . The symbols denote experimental data while the solid lines denote the least-squares fitting line to the modified Curie–Weiss law. (b) Variation in γ with x for the KNN-AS- x ceramics.

that for the A -site complex $(A_1A_2)BO_3$ or B -site complex $A(B_1B_2)O_3$ perovskite ferroelectrics, a large difference in ionic radii of the A - or B -site cations is favorable for the formation of an ordered structure.^{21,22} For the KNN-AS- x ceramics, the differences in ionic radius between the A -site cations ($Ag^+, K^+, \text{ and } Na^+$) and between the B -site cations (Sb^{5+} and Nb^{5+}) are small. As a result, the A - and B -site disorder degrees and the local compositional fluctuation increase, making the ceramics become more relaxorlike and exhibit a diffuse phase transition.^{21,22}

The diffuseness of a phase transition can be determined from the modified Curie–Weiss law $1/\epsilon_r - 1/\epsilon_m = C^{-1}(T - T_m)^\gamma$,^{17–19} where ϵ_m is the maximum value of ϵ_r at the phase transition temperature T_m , γ is the degree of diffuseness, and C is the Curie-like constant. The γ can have a value ranging from 1 for a normal ferroelectric to 2 for an ideal relaxor ferroelectric. Based on the temperature plots of ϵ_r at 10 kHz, the graphs of $\ln(1/\epsilon_r - 1/\epsilon_m)$ versus $\ln(T - T_m)$ for the KNN-AS- x ceramics were plotted, giving the results shown in Fig. 8(a). All the samples exhibit a linear relationship. By least-squares fitting the experimental data to the modified Curie–Weiss law, γ was determined. Figure 8(b) shows the variations in the calculated γ with x for the ceramics. For the ceramic with $x=0$, γ equals to 1.12, revealing the normal ferroelectric characteristics. As x increases, γ increases and then decreases, giving a maximum value of 1.88 at $x=0.08$. This suggests that the addition of AS causes essential changes in the phase transition, and the ceramics become gradually a relaxor ferroelectric and exhibits a broadened transition peak, as shown in Fig. 6.

To demonstrate the practical applicability, the thermal stability of the ceramics was studied. Figure 9 shows the variation in k_p with temperature for the ceramic with x

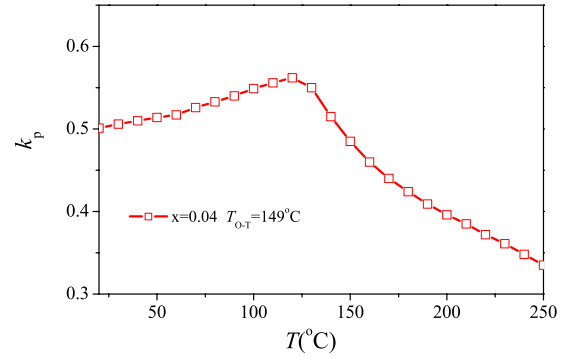


FIG. 9. (Color online) Variation in k_p with temperature for the KNN-AS-0.04 ceramic.

$=0.04$. In general, there is no depoling effect on the ceramics up to T_{O-T} . The observed k_p increases slightly with increasing temperature, and then starts to decrease at temperature close to the T_{O-T} (149 °C). The increase in k_p with temperature should be attributed to the coexistence of the orthorhombic and tetragonal phases near T_{O-T} , which is the major reason for the high piezoelectricity reported in KNN-based systems.^{4–10}

IV. CONCLUSIONS

New lead-free piezoelectric ceramics $(1-x)K_{0.5}Na_{0.5}NbO_3-xAgSbO_3+0.75 \text{ mol } \% \text{ MnO}_2$ have been prepared by a conventional solid-state sintering technique. The ceramics possess a single-phase perovskite structure with orthorhombic symmetry. The addition of $AgSbO_3$ decreases the cubic-tetragonal phase transition temperature (T_C) and the tetragonal-orthorhombic phase transition temperature (T_{O-T}) of the ceramics. Probably due to the strong covalence and small ionic radius of Sb , the ceramics become softened, resulting in significant improvements in ferroelectric and piezoelectric properties. The ceramics with $x=0.03–0.10$ exhibit excellent piezoelectric properties: $d_{33}=130–216 \text{ pC/N}$, $k_p=0.44–0.51$, and $k_t=0.40–0.52$. The ceramics also exhibit a good thermal stability up to the high T_{O-T} .

ACKNOWLEDGMENTS

This work was supported by the Postdoctoral Fellowship grant (G-YX98) of The Hong Kong Polytechnic University.

- ¹R. E. Jaeger and L. Egerton, *J. Am. Ceram. Soc.* **45**, 209 (1962).
- ²L. Egerton and D. M. Dillom, *J. Am. Ceram. Soc.* **42**, 438 (1959).
- ³Z. S. Ahn and W. A. Schulze, *J. Am. Ceram. Soc.* **70**, C18 (1987).
- ⁴Y. Guo, K. Kakimoto, and H. Ohsato, *Appl. Phys. Lett.* **85**, 4121 (2004).
- ⁵R. Zuo, X. Fang, and C. Ye, *Appl. Phys. Lett.* **90**, 092904 (2007).
- ⁶C. W. Ahn, H. C. Song, S. Nahm, S. H. Park, K. Uchino, S. Priya, H. G. Lee, and N. K. Kang, *Jpn. J. Appl. Phys., Part 2* **44**, L1361 (2005).
- ⁷R. Wang, R. Xie, K. Hanada, K. Matsusaka, H. Bando, and M. Itoh, *Phys. Status Solidi A* **202**, R57 (2005).
- ⁸Y. Guo, K. Kakimoto, and H. Ohsato, *Mater. Lett.* **59**, 241 (2005).
- ⁹D. Lin, K. W. Kwok, and H. L. W. Chan, *J. Appl. Phys.* **101**, 074111 (2007).
- ¹⁰D. Lin, K. W. Kwok, and H. L. W. Chan, *Appl. Phys. A: Mater. Sci. Process.* **91**, 167 (2008).
- ¹¹Y. Saito, H. Takao, T. Tani, T. Nonoyama, K. Takatori, T. Homma, T. Nagaya, and M. Nakamura, *Nature (London)* **432**, 84 (2004).
- ¹²D. Lin, K. W. Kwok, and H. L. W. Chan, *J. Phys. D* **41**, 045401 (2008).

- ¹³M. Matsubara, K. Kikuta, and S. Hirano, *J. Appl. Phys.* **97**, 114105 (2005).
- ¹⁴D. Lin, K. W. Kwok, and H. L. W. Chan, *Mater. Chem. Phys.* **109**, 455 (2008).
- ¹⁵B. Jaffe, W. R. Cook, and H. Jaffe, *Piezoelectric Ceramics* (Academic, London, 1971), p. 193.
- ¹⁶S. Saïd and J. P. Mercurio, *J. Eur. Ceram. Soc.* **21**, 1333 (2001).
- ¹⁷C. Karthik, N. Ravishankar, K. B. R. Varma, M. Maglione, R. Vondermuhl, and J. Etourneau, *Appl. Phys. Lett.* **89**, 042905 (2006).
- ¹⁸S. Shannigrahi, P. N. P. Choudary, H. N. Acharya, and T. P. Sinha, *J. Phys. D* **32**, 1539 (1999).
- ¹⁹K. Uchino, S. Nomura, L. E. Cross, S. J. Tang, and R. E. Newnham, *J. Appl. Phys.* **51**, 1142 (1980).
- ²⁰Y. Guo, K. Kakimoto, and H. Ohsato, *Solid State Commun.* **129**, 279 (2004).
- ²¹N. Setter and L. E. Cross, *J. Mater. Sci.* **15**, 2478 (1980).
- ²²N. Setter and L. E. Cross, *J. Appl. Phys.* **51**, 4356 (1980).